Water Science & Technology

Water Science & Technology Vol 85 No 6, 1754 doi: 10.2166/wst.2022.066

Study on the cross-flow ultrafiltration of mixtures of macromolecular organic and inorganic salts

Tingting Xu[a,b], Jie Song[a,b,*] and Guangli Xiu[a,b]

[a] Shanghai Environmental Protection Key Laboratory for Environmental Standard and Risk Management of Chemical Pollutants, School of Resources & Environmental Engineering, East China University of Science and Technology, Shanghai 200237, China
[b] State Environmental Protection Key Lab of Environmental Risk Assessment and Control on Chemical Processes, School of Resources & Environmental Engineering, East China University of Science and Technology, Shanghai 200237, China
*Corresponding Author. E-mail: jiesong@ecust.edu.cn

ABSTRACT

Ultrafiltration (UF) has been widely applied to water treatment in the past few decades, but severe membrane fouling is one of the most significant obstacles for its further development. In reality, the constituents of feed water are complex, and the fouling behavior could be different from that induced by a single foulant. In this study, the membrane fouling induced by mixed organic foulant (sodium alginate, SA) and inorganic ions under various conditions were investigated. The effects of ion concentration and valence on the combined fouling as well as the rejection performance were examined. The results showed that compared to SA alone, the presence of inorganic ions could aggravate the organic fouling of UF membranes significantly. The fouling became more severe as the ion concentration increased. Also, ions with higher valence tended to exacerbate the fouling compared with monovalent ions. It was also found that the existence of inorganic ions had negligible effects on the rejection of organic molecules, however, the rejection of salts can be improved because of the organic matter. In addition, the analysis of the classic fouling models showed that the complete blocking model is the main fouling mechanism of the mixed SA and inorganic salts.

Key words: inorganic ion, membrane fouling, sodium alginate, ultrafiltration

HIGHLIGHTS

- Investigated the membrane fouling induced by mixed organic foulant and inorganic ions under various conditions.
- Examined the ion concentration and valence on the membrane fouling as well as the rejection performance.
- The presence of inorganic ions will significantly aggravate the organic fouling of membranes.
- Complete pore blocking is the main fouling mechanism.

GRAPHICAL ABSTRACT

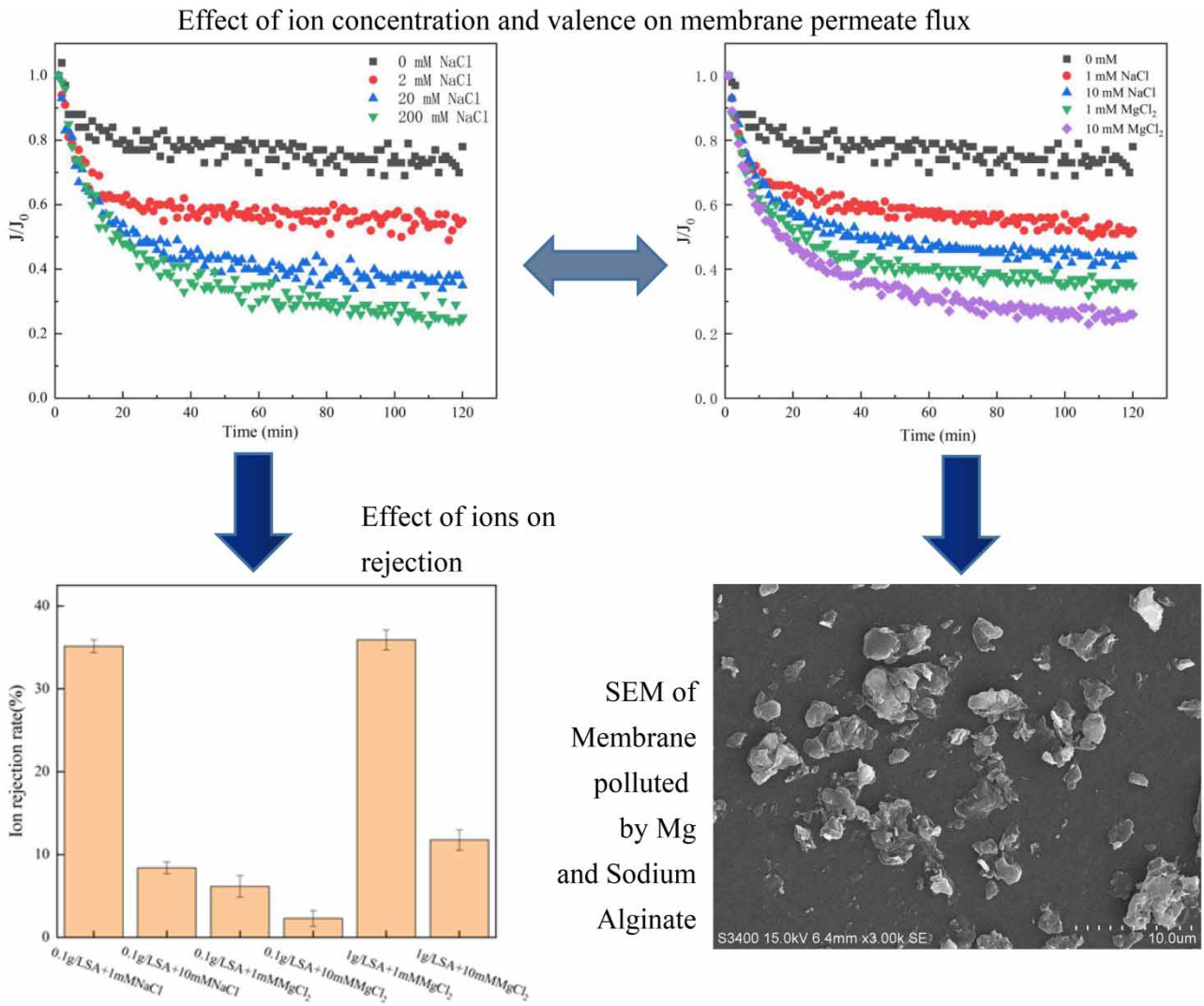

1. INTRODUCTION

With the shortage of water resources and serious pollution problems, more and more attention has been paid to wastewater recycling and resource utilization (Qu *et al.* 2012; Obotey Ezugbe & Rathilal 2020). Membrane technology has been developed rapidly and been applied to various fields such as wastewater treatment, separation and purification at this time (Conidi *et al.* 2017). Ultrafiltration (UF) technology has been widely used in advanced sewage treatment, seawater desalination and food, pharmaceutical and biotechnology industries (Doan & Lai 2021) due to its advantages of high efficiency, low energy consumption, and no secondary pollution (Lafi *et al.* 2018; Cai *et al.* 2021). However, the problem of ultrafiltration membrane fouling in actual operation is one of the main bottlenecks that limits its further development (Jermann *et al.* 2008; Zhu *et al.* 2013; Dhakal *et al.* 2018).

In the past, many studies have been conducted on the analysis of the fouling mechanism of ultrafiltration membranes, however, most of them focused on single pollutants (Goh *et al.* 2018). For example, Nilson and DiGiano (Nilson & DiGiano 1996) and Lin *et al.* (2000) studied the influence of hydrophilicity of organic matter on membrane fouling behavior. Zydeny *et al.* (Carroll *et al.* 2000) investigated the effect of molecular weight of organic matter on membrane fouling and concluded that the membrane fouling caused by organic matter with a larger molecular weight was more severe. In the actual operation process, the water to be treated is complex, which normally contains different types of pollutants (Shi *et al.*

2012). Studies have shown that the membrane fouling behavior of mixed pollutants could be different from that induced by a single pollutant (Guo *et al.* 2012; Liu & Mi 2012).

Compared to fouling by a single pollutant, there are relatively fewer studies on the membrane fouling with the simultaneous presence of both inorganic and organic pollutants, and no unified conclusion has been obtained (Yin *et al.* 2020). Some studies have found that compared with a single pollutant, inorganic–organic pollutants have a significant synergistic effect when they exist simultaneously, which will aggravate membrane fouling. For example, Jermann *et al.* (2007) found that the presence of Ca^{2+} induced an increase in the interaction with alginate molecules, which causes a flux decline. Corbatón-Báguena *et al.* (2015) also observed a similar phenomenon. The mixture of $CaCl_2$ and BSA showed more serious membrane fouling than BSA alone. Tian *et al.* (2013) investigated the fouling behavior of different natural organic matter (NOM) molecules and microparticles on UF membranes, and found that for all NOM models, significant synergistic pollution effects can be observed between organic pollutants and particles. By contrast, some studies have found that the coexistence of inorganic–organic pollutants could significantly reduce the membrane fouling, which is accompanied by a decrease in the rate of membrane fouling. For example, Xiong *et al.* (2019) found that the addition of Al-based flocculant could effectively alleviate the membrane fouling caused by organic matters and increase the permeate flux. Chen *et al.* (2015) studied the effects of iron on the structure and filterability of calcium alginate fouling layers, and the results showed that iron content higher than 30% can improve the filterability of the fouling layer and reduce membrane fouling. Ma *et al.* (2014) also found a similar situation, in the case of high dose of iron salt, the ultrafiltration membrane fouling caused by alginate was significantly reduced. In general, the fouling behavior of mixed pollutants is more complicated than that of a single pollutant, and the fouling mechanism under different conditions is still under investigation (Schulz *et al.* 2016). Therefore, revealing the membrane fouling behavior under the coexistence of inorganic and organic pollutants is meaningful to explore the membrane fouling in real operation processes.

Alginate is widely used as a model foulant as its behavior is similar to that of NOM and it is ubiquitous in natural water bodies (Guo *et al.* 2020). Sodium alginate (SA) is a polysaccharide carbohydrate extracted from brown algae kelp or *Sargassum*, and it has been widely adopted in the study of membrane fouling (Lee & Mooney 2012; Cao *et al.* 2017; Tanna & Mishra 2019; Cao *et al.* 2020). In this study, SA was applied as the organic foulant, and NaCl and $MgCl_2$ as the inorganic salts. The effects of some other inorganic ions which form flocs with alginate (such as Ca^{2+}, Al^{3+} and Fe^{3+}) were not examined in the present study. In this study, the membrane filtration performance of cross-flow ultrafiltration under various operating conditions was studied, and the membrane fouling behavior induced by mixed foulants were investigated. The effects of ion concentration and valence on the membrane fouling were examined through both the macroscopic and microscopic aspects. Moreover, the UF membrane fouling of mixture was analyzed by using the classical fouling models.

2. MATERIALS AND METHODS

2.1. Membrane material and chemical agents

In this study, a flat-sheet ultrafiltration membrane purchased from RisingSun Membrane Technology (Beijing) Co., Ltd was used (model: UE005), and the material was polyethersulfone (PES). The molecular weight cut-off (MWCO) of the membrane is 5,000 Da and the thickness of the membrane is 0.22 mm. The PES ultrafiltration membrane has a three-dimensional mesh sponge structure, which can not only ensure relatively high water flux, but also maintain high filtration accuracy (Li *et al.* 2020).

Before the filtration experiment, the membrane was soaked in deionized water for at least 24 hours, and rinsed by deionized water three times to remove impurities on the membrane surface. All membrane samples were stored in the dark at 4 °C until use to prevent the growth of bacteria.

All chemical reagents used in this study were analytical grade, and were purchased from Shanghai Titan Technology Co., Ltd, including NaCl, $MgCl_2$, and alginate (SA, Mw = 120,000–190,000; Viscosity: 200–500 mPa.s). Deionized (DI) water (resistivity $\geq$ 18.2 MΩ) was obtained by purifying tap water for laboratory use for all experiments.

2.2. UF membrane filtration experiments

2.2.1. Experimental setup

The schematic diagram of the experimental setup is shown in Figure 1. A cross-flow membrane cell made of Plexiglas was used to house the membrane, and the effective filtration area of the membrane was 54 cm^2. A Plexiglas container with the volume of 20 L was used as a feed tank, and the feed was pumped into the membrane cell through a peristaltic pump

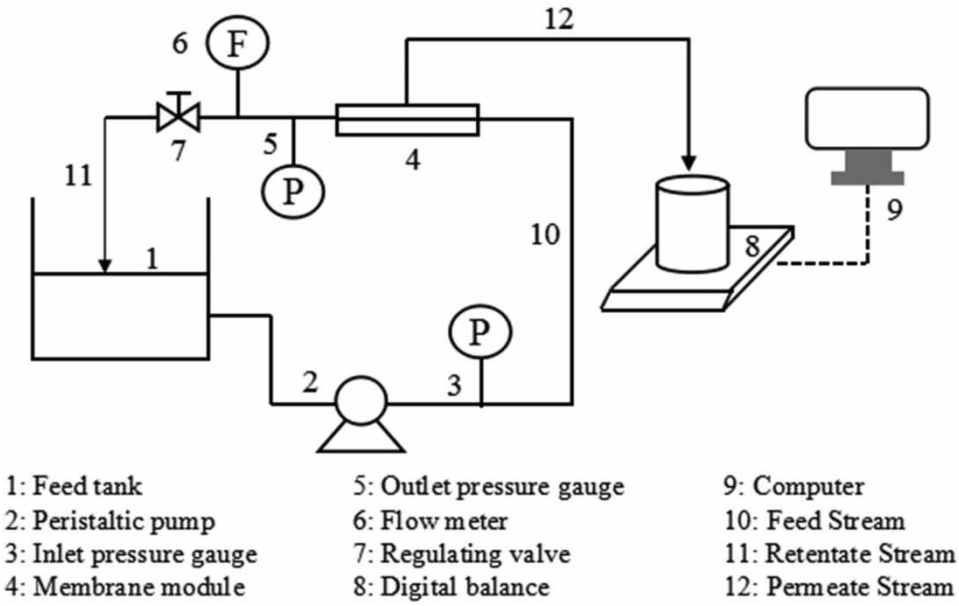

Figure 1 | Schematic diagram of experimental setup.

(Longer Pump, WT600-2 J). The transmembrane pressure and cross-flow velocity of the system can be controlled by adjusting the rotation speed of the peristaltic pump and the needle valve at the exit of the retentate. All the pressure and flow rate data can be monitored online, and transferred to a computer for storage. The permeate flow rate was measured by an electronic balance (Chengdu Presun Electronics Co., Ltd, HT-1500FW), which was connected to the computer to obtain the real-time weight of the permeate. The computer records the weight every one minute, and the permeate flux is calculated according to the following equation:

$$J = \frac{m_t - m_{t-1}}{A_m \times t} \quad (t = 1, 2, 3 \ldots..120) \tag{1}$$

where J ($g \cdot min^{-1} \cdot m^{-2}$) is the permeate flux of filtering t minutes; m_t and m_{t-1} (g) is the corresponding weight when filtering t and $t - 1$ minutes, A_m (m^2) is the effective filtration area of the membrane and t (min) is the time interval between readings.

2.2.2. Membrane filtration experiments

For each experiment, DI water was filtered by the membrane for 30 minutes under the experimental conditions for membrane compression, and the permeate flux of pure water was used as the initial flux J_0. The feed solution with specific concentration was prepared by adding certain amounts of SA and inorganic salts into the DI water and mixed homogeneously before being pumped into the system. Each experiment lasted for at least 120 minutes, and the feed conditions (i.e. pressure and flow rate) and permeate flow rate were monitored continuously during the experiment. For membrane fouling analysis, the fouled membranes were removed from the cell, dried and sealed stored at 4°C after the experiment.

In this study, the effects of organic–inorganic mixture concentration, ion strength and valence on the cross-flow ultrafiltration performance and fouling behavior were studied and analyzed. All experiments were carried out at a room temperature of 25 ± 1 °C.

2.2.3. Other analytical measurements

Besides the examination of the permeate flux, the rejection performance was investigated as well. The German Liqui TOC instrument was used to determine the TOC of the permeate sample. The conductivity of the sample was determined by using a conductivity meter (ULTRAMETER II™ $6PFC^E$). A scanning electron microscope (SEM, Hitachi, Japan, S-3400N) was applied to characterize the surface morphology of the membrane and the foulant layer.

2.3. Model analysis for UF membrane fouling

The classic fouling models introduced by M. Cinta Vincent Vela (Vincent Vela *et al.* 2009) are used in this study to better understand the membrane fouling induced by mixed pollutants. The corresponding model diagrams and equations are shown in Table 1. According to previous studies, the complete blocking model assumes that every solute molecule deposited on the membrane surface completely blocks a membrane pore and does not overlap with each other, that is, a molecule will never precipitate on the previously deposited molecules on the membrane surface. Therefore, a single cake layer is formed on the surface of the membrane. The intermediate blocking model is similar to the completely blocking model to a certain extent, however, this model believes that a membrane pore is not necessarily blocked by a solute molecule, and there is a probability that the solute molecule falls on top of other molecules. The standard blocking model occurs when the solute molecules are smaller than the pore diameter of the membrane. It assumes that the solute molecules enter the membrane pores and deposit on the inner surface of the membrane pores, resulting in a reduction in the membrane pore size. The cake filtration model assumes that the solutes do not enter the membrane pores but form a cake layer on the membrane surface, and the particles are deposited on the particles deposited in the early stage.

Among them, J_0 represents the initial permeate flux (m/s), J_s represents the equilibrium permeate flux (m/s), the parameter K_i represents the total volume per unit permeated through the membrane when the membrane surface is fouled (1/m), K_s represents the volume of solids retained per unit permeating the membrane ($10^3/s^{0.5}\ m^{0.5}$), K_g represents the ratio between the characteristics of the fouling layer and the characteristics of the not fouling membrane (s/m^2).

3. RESULTS AND DISCUSSION

3.1. Membrane filtration performance of single alginate

In this study, the effects of operating conditions (i.e. feed concentration, transmembrane pressure and cross-flow velocity) on the membrane fouling behavior induced by alginate alone were studied first.

Table 1 | Schematic diagrams and equations of classical fouling models

	Equation	Schematic diagram
Complete blocking model	$J = J_s + (J_0 - J_s)e^{-K_i J_0 t}$	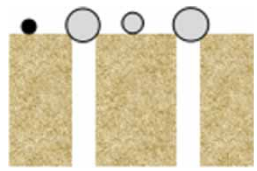
Intermediate blocking model	$J = \frac{J_0 J_s e^{K_i J_s t}}{J_s + J_0(e^{K_i J_s t} - 1)}$	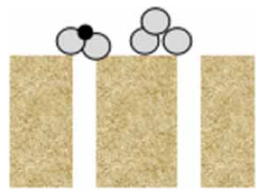
Standard blocking model	$J = \frac{4J_0}{(2 + J_0^{1/2} K_s t)^2}$	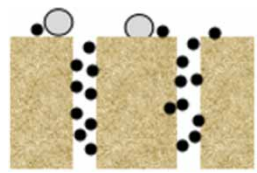
Cake filtration model	$t = \frac{1}{K_g J_s^2} \ln\left[\left(\frac{J}{J_0}\frac{J_0 - J_s}{J - J_s}\right) - J_s\left(\frac{1}{J} - \frac{1}{J_0}\right)\right]$	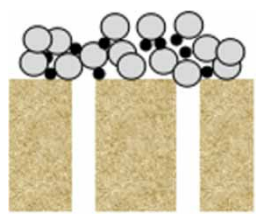

Figure 2 shows the decline of permeate flux at different concentration of SA. The cross-flow velocity was fixed at 10 cm/s, and the transmembrane pressure was 150 kPa. For the SA solution with low concentration (i.e. 20 mg/L), the flux reduction was small and J/J_0 can be maintained close to 1, which suggests that the fouling is slight under such low feed concentration. As the concentration increased, the permeate flux induced by SA declined sharply, and the drop occurred within the first few minutes after the filtration started. The specific flux decreased to 0.74 and 0.35 at concentrations of 0.1 g/L and 1 g/L, respectively. It is worth noting that when the concentration is 1 g/L, the membrane flux drops rapidly at the beginning of filtration and gradually reaches a stable value.

The effect of transmembrane pressure on the membrane filtration of 1 g/L SA is shown in Figure 3, where the cross-flow velocity was fixed at 10 cm/s. It can be seen that, as the pressure increased, the relative permeate flux decreased from 0.43 at 100 kPa to 0.35 and 0.34, at 150 kPa and 200 kPa, respectively. This implies that the pressure increase tends to aggravate the membrane fouling, however, the variation induced by pressure is relatively small for cross-flow ultrafiltration.

The permeate flux variation under different cross-flow velocity is illustrated in Figure 4, where the pressure was 200 kPa and the feed concentration was 1 g/L. It can be seen that the membrane specific flux increased from 0.34 of 10 cm/s to

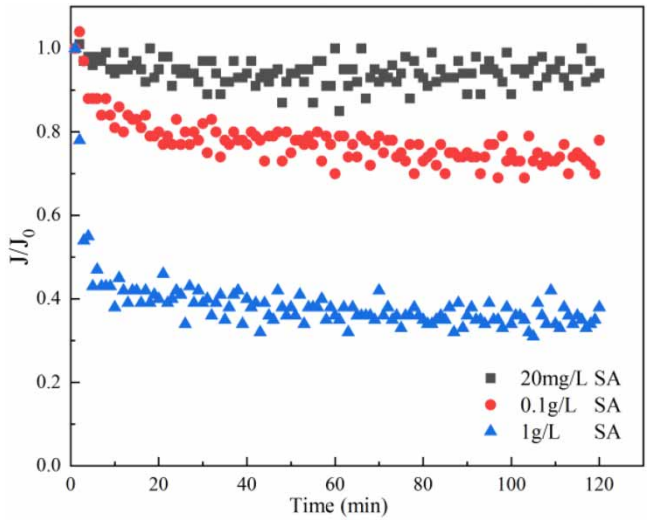

Figure 2 | Effect of feed concentration on membrane filtration of single SA with cross-flow velocity of 10 cm/s and pressure of 150 kPa.

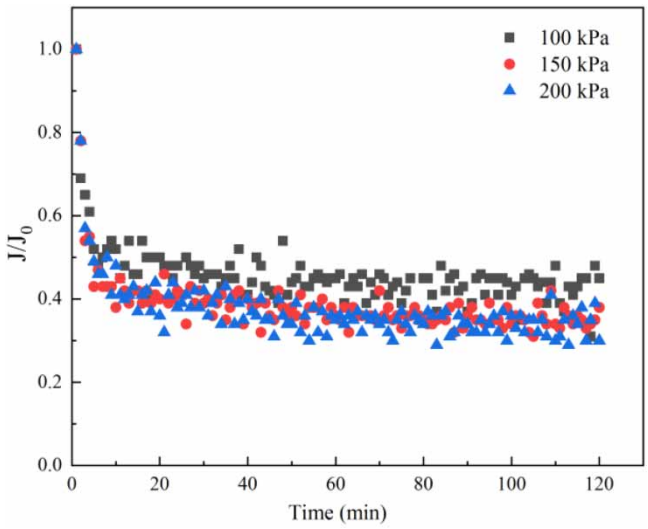

Figure 3 | Effect of transmembrane pressure on single SA membrane filtration with concentration of 1 g/L and cross-flow velocity of 10 cm/s.

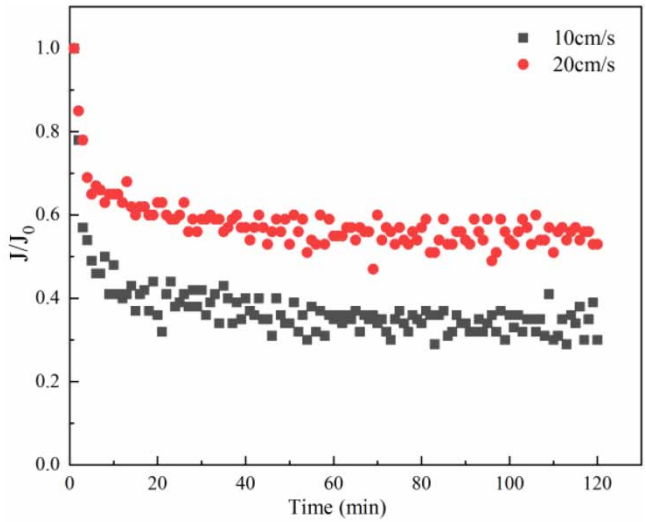

Figure 4 | Effect of cross-flow velocity on single SA membrane filtration with concentration of 1 g/L and pressure of 200 kPa.

0.55 of 20 cm/s. This is because that higher cross-flow velocity will increase the shear stress on the membrane surface, which is favorable for fouling mitigation.

3.2. Effect of inorganic concentration on the membrane filtration performance

In this study, the membrane fouling behavior induced by alginate macromolecules in the presence of different inorganic ions (Na^+ and Mg^{2+}) was investigated. Figure 5 shows the filtration performance under various ionic strength by adding additional NaCl to the SA solution. The cross-flow velocity was fixed at 10 cm/s, the transmembrane pressure was fixed at 150 kPa, and the SA concentration was 0.1 g/L. It can be seen that the permeate flux decreases as the NaCl concentration increases. As the NaCl concentration increased from 0 to 200 mM, the relative permeate flux dropped from 0.74 to 0.27 rapidly. This suggests that the ionic strength will affect the membrane filtration performance in a negative way. The possible explanation is that the physical properties of alginate can be influenced by the ionic strength of the solution. Compared with pure SA solution, the addition of monovalent cations (Na^+) causes the electric double layer around the alginate molecules to be compressed by higher ionic strength. Hence, the alginate molecules become more coiled and aggravate the fouling of the membrane. Previous research also reported a similar phenomenon, indicating that monovalent cations can cause the aggregation of other organic substances, thereby exacerbating membrane fouling, such as fulvic acid (Tang *et al.* 2014) and fullerenes (Zhang

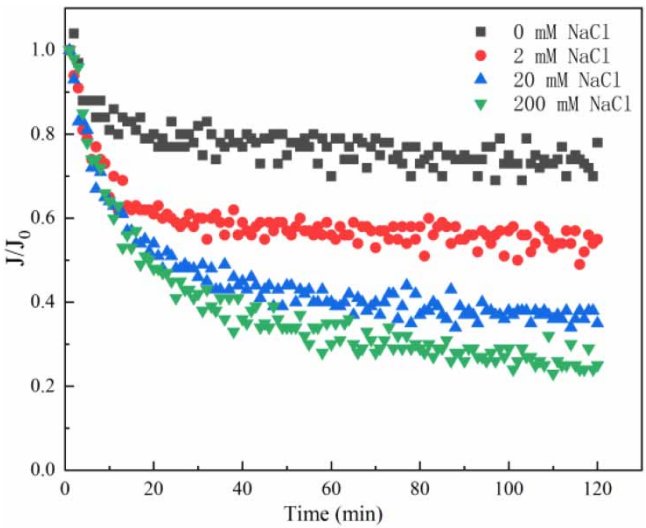

Figure 5 | Effect of concentration of Na^+ on membrane filtration with 0.1 g/L of SA under the operating conditions of 150 kPa and 10 cm/s.

et al. 2014). The filtration performance of alginate and Mg^{2+} is similar, however, the flux keeps almost unchanged after the Mg^{2+} concentration reaches 10 mM.

3.3. Effect of ion valence on the membrane filtration performance

In order to understand the effect of ion valence on the membrane fouling, the filtration performance of SA solution with monovalent and divalent inorganic salts (i.e. Na^{+} and Mg^{2+}) were investigated as shown in Figure 6, where the SA concentration was 0.1 g/L, transmembrane pressure 150 kPa and cross-flow velocity 20 cm/s. It can be seen from the figure that at an ion concentration of 1 mM, the relative permeate flux dropped from the initial 0.74 to 0.54 and 0.36 for Na^{+} and Mg^{2+}, respectively. At an ion concentration of 10 mM, the permeate flux dropped to 0.44 and 0.26 for Na^{+} and Mg^{2+}, respectively. It can be seen from the figure that compared with Na^{+}, a lower dosage of Mg^{2+} can induce a larger flux decline. With the same concentration, Mg^{2+} tends to induce more severe membrane fouling compared to Na^{+}. The possible reason is that Mg^{2+} can be linked with the carboxyl groups of SA molecules, this leads to a 'bridging' effect and increases the particle size (Lee & Elimelech 2006; Ma *et al.* 2018).

3.4. Membrane rejection of mixed organic–inorganic solution

Besides the permeate flux, the membrane rejection of mixed organic–inorganic solutions was investigated. It was found that the rejection rate of alginate (TOC) is almost not affected by presence of inorganic ions and is higher than 98%. The reason is that the molecular weight of SA is much higher than the MWCO of the membrane, and most of the macromolecules can be removed by the membrane.

The rejection of inorganic ions varies at different conditions. The rejection of pure salts is almost negligible as the size of ions is much smaller than that of the UF membrane pores. However, with the presence of alginate, both the rejection of NaCl and $MgCl_2$ was improved significantly. The rejection of inorganic ions under various conditions is compared in Figure 7. The cross-flow velocity was 20 cm/s, and the transmembrane pressure was 150 kPa. It can be seen that when the concentration of SA is the same, the higher ion concentration leads to a lower rejection rate, which shall be attributed to the super saturation of SA interaction sites for inorganic ions. It also can be seen that the rejection rate of Na^{+} is higher than that of Mg^{2+} when the ion concentration is identical. The reason is that under the same concentration of SA, more Na^{+} ions can be bound by the SA molecules and be rejected by the UF membrane.

3.5. Fouling analysis of organic–inorganic mixture

To analyze the fouling mechanism in the absence and presence of ions, the variation of permeate flux was further modeled with the four theoretical models exhibited in Table 1. The regression results and corresponding coefficient R^2 were computed,

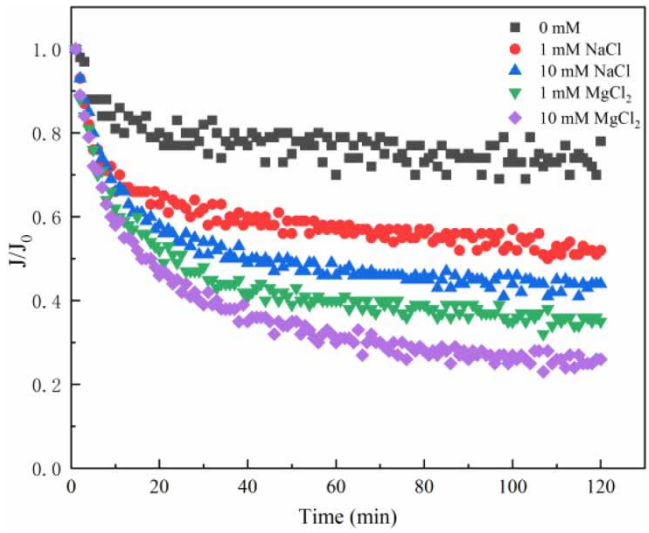

Figure 6 | Effect of ion valence on the membrane filtration with 0.1 g/L of SA under the operating conditions of 150 kPa and 20 cm/s.

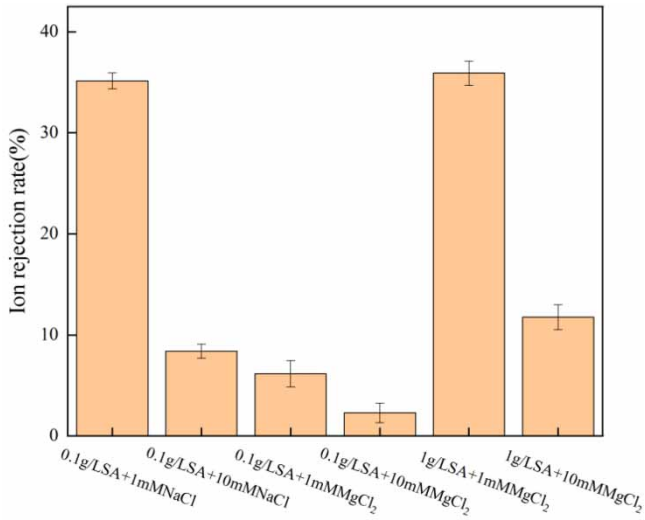

Figure 7 | Membrane rejection rate of ions of different mixtures under the operating conditions of 150 kPa and 20 cm/s.

which depicted the fouling behaviors with varied underlying mechanisms. The goodness of fit (R^2) of each model of SA solutions with different sodium chloride and magnesium chloride concentrations was calculated.

The coefficients of determination are shown in Table 2. The results showed that when the SA concentration is high (i.e. 1 g/L), the complete blocking model is the best fit model for membrane fouling induced by both Na^+ and Mg^{2+} ($R^2 > 0.94$), which suggests that the formation of UF fouling is mainly due to the complete blocking mechanism at high organic concentration, regardless of the ion concentration. When the SA concentration is relatively lower (i.e. 0.1 g/L), both the complete blocking and the intermediate blocking models have a good correlation ($R^2 > 0.94$). This finding is different from Ma *et al.* (2018), where the cake layer model was found to suit the dead-end UF of HA and inorganic mixture the most.

To gain more insights into the fouling mechanism induced by the mixture of alginate and inorganic salts, a morphological study of the fouled membranes was performed as shown in Figure 8. For the mixture of SA and Na^+, a relatively homogeneous fouling layer was formed on top of the membrane surface (Figure 8(d)), while for the mixture of SA and Mg^{2+}, obvious particles can be observed which blocked the membrane (Figure 8(f)).

4. CONCLUSIONS

In the present study, the cross-flow ultrafiltration performance of combined organic matter and multiple inorganic ions has been investigated experimentally. It was found that the membrane fouling occurs in the early stage rapidly due to the large

Table 2 | Coefficients of determination (R^2) of classic pollution model for membrane fouling

	R^2			
Foulant	**Complete blocking model**	**Intermediate blocking model**	**Standard blocking model**	**Cake filtration model**
1 g/LSA	0.9204	0.8981	0.8546	0.3182
1 g/LSA + 1 mM NaCl	0.9556	0.9442	0.9178	0.1833
1 g/LSA + 10 mM NaCl	0.9571	0.9399	0.6394	0.0174
1 g/LSA + 1 mM $MgCl_2$	0.9487	0.9269	0.1776	0.1962
1 g/LSA + 10 mM $MgCl_2$	0.9442	0.9263	0.8299	0.3321
0.1 g/LSA	0.8200	0.9304	0.8390	0.5122
0.1 g/LSA + 1 mM NaCl	0.9461	0.9492	0.8662	0.2613
0.1 g/LSA + 10 mM NaCl	0.9753	0.9837	0.6092	0.4268
0.1 g/LSA + 1 mM $MgCl_2$	0.9759	0.9832	0.5832	0.4861
0.1 g/LSA + 10 mM $MgCl_2$	0.9614	0.9754	0.8239	0.5031

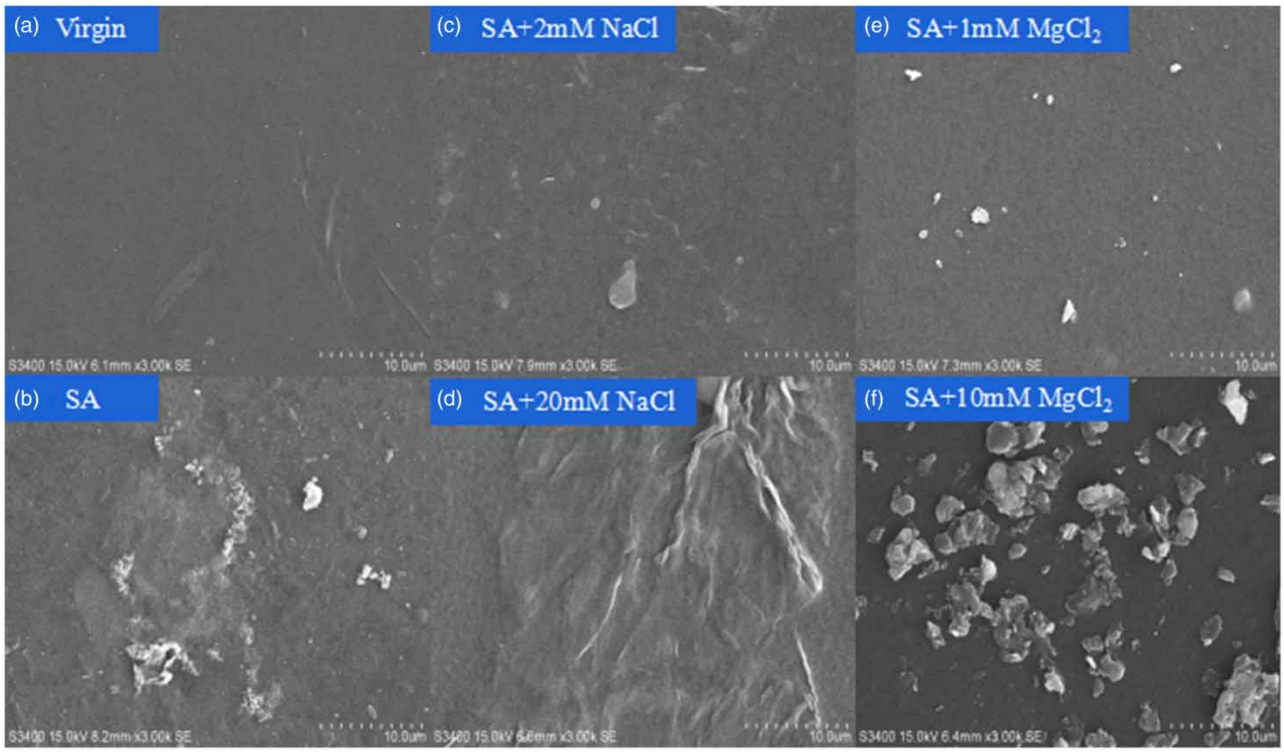

Figure 8 | SEM images of fouled membranes after filtration of 1 g/L SA solutions with different ion concentrations. The images were all captured with the magnification of 3000.

molecular size of alginate. Compared to single alginate solution, existence of inorganic ions will aggravate the membrane fouling significantly, and the severity of fouling increases with the ion concentration. Moreover, Mg^{2+} ions are more likely to cause more serious fouling than Na^{+} ions. The reason is that the monovalent inorganic ions tend to compress the SA electric double layer, while the divalent inorganic ions increase the particle size mainly through the 'bridging' effect. It was also found that when both the organic and inorganic pollutants exist, the rejection of organic molecules was not affected, however, the rejection of inorganic salts can be improved significantly. In addition, by analyzing the experimental results, the complete blocking model is demonstrated to be the most suitable model for the membrane fouling induced by the mixture of alginate and inorganic salts of cross-flow ultrafiltration.

ACKNOWLEDGEMENTS

This work was sponsored by the Shanghai sailing program (20YF1409700).

DATA AVAILABILITY STATEMENT

All relevant data are included in the paper or its Supplementary Information.

REFERENCES

Cai, W., Gao, Z., Yu, S., Lv, M., Shi, Y. & Wang, J. 2021 New insights into membrane fouling formation during ultrafiltration of organic wastewater with high salinity. *Journal of Membrane Science* **635**, 119446.

Cao, D. Q., Hao, X. D., Wang, Z., Song, X., Iritani, E. & Katagiri, N. 2017 Membrane recovery of alginate in an aqueous solution by the addition of calcium ions: analyses of resistance reduction and fouling mechanism. *Journal of Membrane Science* **535**, 312–321.

Cao, D., Jin, J., Wang, Q., Song, X., Hao, X., Iritani, E. & Katagiri, N. 2020 Ultrafiltration recovery of alginate: membrane fouling mitigation by multivalent metal ions and properties of recycled materials. *Chinese Journal of Chemical Engineering* **28** (11), 2881–2889.

Carroll, T., King, S., Gray, S. R., Bolto, B. A. & Booker, N. A. 2000 The fouling of microfiltration membranes by NOM after coagulation treatment. *Water Research* **34** (11), 2861–2868.

Chen, X. D., Yang, H. W., Liu, W. J., Wang, X.-M. & Xie, Y. F. 2015 Filterability and structure of the fouling layers of biopolymer coexisting with ferric iron in ultrafiltration membrane. *Journal of Membrane Science* **495**, 81–90.

Conidi, C., Cassano, A., Caiazzo, F. & Drioli, E. 2017 Separation and purification of phenolic compounds from pomegranate juice by ultrafiltration and nanofiltration membranes. *Journal of Food Engineering* **195**, 1–13.

Corbatón-Báguena, M. J., Álvarez-Blanco, S. & Vincent-Vela, M. C. 2015 Fouling mechanisms of ultrafiltration membranes fouled with whey model solutions. *Desalination* **360**, 87–96.

Dhakal, N., Salinas-Rodriguez, S. G., Ouda, A., Schippers, J. C. & Kennedy, M. D. 2018 Fouling of ultrafiltration membranes by organic matter generated by marine algal species. *Journal of Membrane Science* **555**, 418–428.

Doan, N. T. T. & Lai, Q. D. 2021 Ultrafiltration for recovery of rice protein: fouling analysis and technical assessment. *Innovative Food Science & Emerging Technologies* **70**, 102692.

Goh, P. S., Lau, W. J., Othman, M. H. D. & Ismail, A. F. 2018 Membrane fouling in desalination and its mitigation strategies. *Desalination* **425**, 130–155.

Guo, W., Ngo, H. H. & Li, J. 2012 A mini-review on membrane fouling. *Bioresource Technology* **122**, 27–34.

Guo, D., Xiao, Y., Li, T., Zhou, Q., Shen, L., Li, R., Xu, Y. & Lin, H. 2020 Fabrication of high-performance composite nanofiltration membranes for dye wastewater treatment: mussel-inspired layer-by-layer self-assembly. *Journal of Colloid and Interface Science* **560**, 273–283.

Jermann, D., Pronk, W., Meylan, S. & Boller, M. 2007 Interplay of different NOM fouling mechanisms during ultrafiltration for drinking water production. *Water Research* **41** (8), 1713–1722.

Jermann, D., Pronk, W. & Boller, M. 2008 Mutual influences between natural organic matter and inorganic particles and their combined effect on ultrafiltration membrane fouling. *Environmental Science & Technology* **42** (24), 9129–9136.

Lafi, R., Gzara, L., Lajimi, R. H. & Hafiane, A. 2018 Treatment of textile wastewater by a hybrid ultrafiltration/electrodialysis process. *Chemical Engineering and Processing – Process Intensification* **132**, 105–113.

Lee, S. & Elimelech, M. 2006 Relating organic fouling of reverse osmosis membranes to intermolecular adhesion forces. *Environmental Science & Technology* **40** (3), 980–987.

Lee, K. Y. & Mooney, D. J. 2012 Alginate: properties and biomedical applications. *Progress in Polymer Science* **37** (1), 106–126.

Li, B., He, X., Wang, P., Liu, Q., Qiu, W. & Ma, J. 2020 Opposite impacts of K_{+} and Ca_{2+} on membrane fouling by humic acid and cleaning process: evaluation and mechanism investigation. *Water Research* **183**, 116006.

Lin, C. F., Lin, T. Y. & Hao, O. J. 2000 Effects of humic substance characteristics on UF performance. *Water Research* **34** (4), 1097–1106.

Liu, Y. & Mi, B. 2012 Combined fouling of forward osmosis membranes: synergistic foulant interaction and direct observation of fouling layer formation. *Journal of Membrane Science* **407–408**, 136–144.

Ma, B., Yu, W., Liu, H. & Qu, J. 2014 Comparison of iron (III) and alum salt on ultrafiltration membrane fouling by alginate. *Desalination* **354**, 153–159.

Ma, B., Ding, Y., Li, W., Hu, C., Yang, M., Liu, H. & Qu, J. 2018 Ultrafiltration membrane fouling induced by humic acid with typical inorganic salts. *Chemosphere* **197**, 793–802.

Nilson, J. A. & DiGiano, F. A. 1996 Influence of NOM composition on nanofiltration. *Journal – American Water Works Association* **88** (5), 53–66.

Obotey Ezugbe, E. & Rathilal, S. 2020 Membrane technologies in wastewater treatment: a review. *Membranes* **10** (5), 89.

Qu, F., Liang, H., Wang, Z., Wang, H., Yu, H. & Li, G. 2012 Ultrafiltration membrane fouling by extracellular organic matters (EOM) of *Microcystis aeruginosa* in stationary phase: influences of interfacial characteristics of foulants and fouling mechanisms. *Water Research* **46** (5), 1490–1500.

Schulz, M., Soltani, A., Zheng, X. & Ernst, M. 2016 Effect of inorganic colloidal water constituents on combined low-pressure membrane fouling with natural organic matter (NOM). *Journal of Membrane Science* **507**, 154–164.

Shi, X., Field, R. & Hankins, N. 2012 Review of fouling by mixed feeds in membrane filtration applied to water purification. *Desalination and Water Treatment* **35** (1–3), 68–81.

Tang, C., He, Z., Zhao, F., Liang, X. & Li, Z. 2014 Effects of cations on the formation of ultrafiltration membrane fouling layers when filtering fulvic acid. *Desalination* **352**, 174–180.

Tanna, B. & Mishra, A. 2019 Nutraceutical potential of seaweed polysaccharides: structure, bioactivity, safety, and toxicity. *Comprehensive Reviews in Food Science and Food Safety* **18** (3), 817–831.

Tian, J. Y., Ernst, M., Cui, F. & Jekel, M. 2013 Effect of particle size and concentration on the synergistic UF membrane fouling by particles and NOM fractions. *Journal of Membrane Science* **446**, 1–9.

Vincent Vela, M. C., Álvarez Blanco, S., Lora García, J. & Bergantiños Rodríguez, E. 2009 Analysis of membrane pore blocking models adapted to crossflow ultrafiltration in the ultrafiltration of PEG. *Chemical Engineering Journal* **149** (1–3), 232–241.

Xiong, X., Xu, H., Zhang, B., Wu, X., Sun, H., Wang, D. & Wang, Z. 2019 Floc structure and membrane fouling affected by sodium alginate interaction with Al species as model organic pollutants. *Journal of Environmental Sciences (China)* **82**, 1–13.

Yin, Z., Ma, Y., Tanis-Kanbur, B. & Chew, J. W. 2020 Fouling behavior of colloidal particles in organic solvent ultrafiltration. *Journal of Membrane Science* **599**, 117836.

Zhang, L., Zhao, Q., Wang, S., Mashayekhi, H., Li, X. & Xing, B. 2014 Influence of ions on the coagulation and removal of fullerene in aqueous phase. *Science of the Total Environment* **466–467**, 604–608.

Zhu, X., Loo, H.-E. & Bai, R. 2013 A novel membrane showing both hydrophilic and oleophobic surface properties and its non-fouling performances for potential water treatment applications. *Journal of Membrane Science* **436**, 47–56.

First received 5 October 2021; accepted in revised form 7 February 2022. Available online 24 February 2022